Original Article

DOI: 10.5582/bst.2017.01063

Perfusion and drainage difference in the liver parenchyma: Regional plane in segment 6

Hayato Abe, Shintaro Yamazaki*, Masamichi Moriguchi, Tokio Higaki, Tadatoshi Takayama

Department of Digestive Surgery, Nihon University School of Medicine, Tokyo, Japan.

Summary **The differences between the perfusion areas of portal vein and the drainage areas of hepatic vein result in the occurrence of either ischemic or congested areas after liver resection. To elucidate which factors are related to the differences between these areas of segment (S) 6 were therefore investigated. The portal-vein-based and hepatic-vein-based regional planes of S6 were defined using the region-growing and Voronoi tessellation methods in 103 consecutive patients who undergo liver resection. Finally, factors related to the difference between the perfusion and drainage areas of S6 were identified. The S6 regional plane based on the portal was coincident with that of hepatic veins (non-difference group) in 57 patients (55.3%), but was discordant on the ventral side (S6-dominant group) in 43 patients (41.7%) and the dorsal side (S5-dominant group) in 3 patients (3.0%). The presence of a proximal branch of the first portal 6 (S6-dominant group *vs.* non-difference group, 72.1% *vs.* 17.0%, $p < 0.001$) and the presence of an inferior right hepatic vein (S6-dominant group *vs.* non-difference group, 72.1% *vs.* 43.9%, $p = 0.008$) suggested large S6 ventrally. The median volume difference between the perfusion area of the portal vein and drainage area of the hepatic vein in S6 was 73 mL (range: 29-189 mL). In conclusion, preoperative 3D-simulation may enhance the preciseness of anatomic liver resection.**

Keywords: Anatomic liver resection, three-dimensional liver anatomy, regional plane

1. Introduction

Recent advances in three dimensional (3D)-computed tomography (CT) of the liver anatomy have revealed that the perfusion areas of the portal vein and drainage area of the hepatic vein in the same segment did not always coincident (*1-3*). The liver anatomy as defined by Couinaud is the widely accepted clinical anatomy which defined the hepatic veins as one of the major landmarks of each segment (*4,5*). The liver staining method, in which dye is injected into the tumor occupying area of the portal vein, had been accepted as an anatomic liver resection method based on the perfusion area of portal vein (*6*). For precise liver resection, it is necessary to understand that there is a difference of tumor occupying area between the concepts.

The preoperative evaluation in 3D-CT is an ideal approach to understand this difference. However, few reports have so far focused on this essential issue in anatomic liver resection (*7,8*). We investigate which anatomic factors influenced to such differences and how much parenchymal volume was different between the perfusion areas and drainage area of the liver parenchyma.

2. Materials and Methods

2.1. *Patients*

Between October 2013 and September 2014, preoperative 3D reconstruction and volumetric analyses of the liver were performed in 103 consecutive patients who underwent liver resection for hepatocellular carcinoma. All patients had radically resectable

Released online in J-STAGE as advance publication May 8, 2017.

**Address correspondence to:*
Dr. Shintaro Yamazaki, Department of Digestive Surgery, Nihon University School of Medicine 30-1 Ohyaguchikami-chou, Itabashi-ku, Tokyo 173-8610, Japan.
E-mail: yamazaki-nmed@umin.ac.jp

hepatocellular carcinomas; the tumor diameter measured within 50 mm in a single tumor and within 30 mm in multiple tumors. The operative management strategies that are used at our institution have been described elsewhere (*9-12*). Ethics Committee approval was obtained (protocol number: RK-170214-03).

2.2. *Three-dimensional reconstruction protocol*

Three-phase, contrast-enhanced dynamic CT scans (unenhanced and hepatic arterial [37 seconds], portal venous [60 seconds], and liver parenchymal phases [150 seconds]) were obtained using a 16- or 350-detector row scanner (Aquilion 16/ONE; Toshiba Medical Systems, Otawara, Japan). The total dose of nonionic iodinated contrast medium was 630 mgI/kg body weight of iomeprol (350 mgI/mL). Scanning was performed using a 15.0- or 53.0-helical pitch, a table feed speed of 0.75 or 0.5 mm per rotation, a slice thickness of 0.5 mm, and 120 kV on a Volume EC system (Toshiba Corporation, Mie, Japan).

To perform 3D image reconstruction and volumetric measurements, the region-growing and the Voronoi tessellation method software programs (Volume Analyzer SYNAPSE VINCENT, FUJIFILM Corporation, Tokyo, Japan) were used. The 3D liver images were created using a region-growing algorithm.

2.3. *Assessment view and definition of the portal-vein-based and hepatic-vein-based anatomies*

The assessment view in the 3D-liver was defined as follows. First, the rotation angle (θ) between the proximal trunk of the right hepatic vein (RHV) and the median line on the inferior vena cava (IVC) of the horizontal plane of the CT scan was defined as a vertical and frontal view (RHV frontal view) on 3D-simulation (Figure 1a). This distal side of the RHV was extracted when the main trunk of the RHV was fully exposed as long as possible in virtual liver resection. This extracted RHV line was defined as the RHV trunk line. The assessment view was fixed as this RHV trunk line was located in the most dorsal of the 3D-liver.

Next, portal-vein-based S6 was defined as the perfusion area of P6 (Figure 1b), and the cranial-dorsal side from the posterior branch was defined as S6 if there were multiple trunks of P6. The hepatic-vein-based S6 was defined as the drainage area of lateral-dorsal tributaries to the RHV in the region growing method (Figure 1c). When the inferior or middle RHV was present, the drainage area of S6 was measured. The dominancy of the parenchymal volume was defined by the position relationship of the regional plane of portal-vein-based S6 to the main trunk of the RHV: the plane runs ventrally beyond the RHV (S6-dominant group); dorsally beyond the RHV (S5-dominant group) or almost equal (non-difference group).

2.4. *Hepatic vein analysis in the 3D liver*

First, the tributary pattern, thicknesses of the main trunk and second-order tributaries, angles between the IVC and RHV, and the presence of tributaries of the RHV (*i.e.*, inferior or middle RHV) were assessed. Next, the second-order large drainage veins from the right liver to the RHV (V7) and the middle hepatic vein (MHV) (V6 and V8) were assessed.

2.5. *Portal vein analysis in the 3D liver*

Regarding the portal vein, the branch type of the main portal trunk, the length of the second-order portal vein, and the distance from the main portal trunk were assessed in the 3D liver. Next, the lengths of the anterior and posterior branches, the angle between these branches, and the number of P6 branches were assessed. When there were multiple trunks of P6, the entire caudal-dorsal side from the posterior branch was defined as S6. The perfusion area of the entire caudal-ventral side of the anterior portal trunk was defined as S5. S7 or S8 was derived by subtracting S5 or S6. Standard bifurcation of the portal vein was defined as the absence of an abnormally branched right portal vein (*i.e.*, no independent posterior branch), with anterior branches or P8 arising from the left portal trunk (umbilical portion). Anatomical variations of the portal branches were evaluated for the right liver, as described by Couinaud (*1,13*).

The branch patterns of P6 were divided into two types (Figure 2). On the assessment view, the first branch of P6 was branched toward the proximal side of the RHV trunk line (proximal type) or branched distal side (distal type). Finally, the factors related to the dominancy of the hepatic parenchymal volume in S6 were assessed.

2.6. *Volume difference between the portal-vein-based and hepatic-vein-based anatomies in S6*

The parenchymal volume of the portal-vein-based S6 was calculated according to the perfusion area of P6 (Figure 3a), while the parenchymal volume of the hepatic-vein-based S6 was defined by the drainage area of lateral-dorsal tributaries to the RHV (Figure 3b) using the Voronoi tessellation method. These volumes were calculated using the workstation (SYNAPSE VINCENT). Finally, the volume difference between the portal-vein-based and hepatic-vein-based anatomies in S6 was compared.

2.7. *Statistical analysis*

Clinical data were recorded on an Excel (Microsoft) spreadsheet and analyzed using the JMP® 9.0 statistical software package (SAS Institute Inc., Cary, NC, USA). All variables were analyzed using the Mann-Whitney

U test or Fisher's exact test. A *p* value of < 0.05 was considered statistically significant.

3. Results

3.1. *Anatomical characteristics*

In the 103 preoperative patients (male:female ratio, 77:26, and median age, 66 years (range, 41-85 years)), the median rotation angle (θ) used to obtain the RHV frontal view of the RHV trunk line was 83.3 degrees (range, 56.2-97.4 degrees) (Figure 1a). On this RHV frontal view, 46 patients (44.7%) were different to the RHV trunk line on the ventral side (S6-dominant group) in 43 patients (41.7%) and the dorsal side (S5-dominant group) in 3 patients (3.0%). In 57 patients (55.3%), the portal perfusion area agreed with the hepatic drainage area for the RHV trunk line (non-difference group). The S5-dominant segmentation was noted in only 3 patients (3.0%), and further estimation was thus not performed.

3.2. *Tributary pattern of the hepatic vein*

There was no significant difference in the angle of the RHA trunk (θ) for creating the RHV trunk line (80.8 degrees [66.4-95.4] *vs*. 84.2 degrees [56.2-97.4], $p = 0.177$), the median thickness of the RHV (6.5 mm [2.8-11.2] *vs*. 6.6 mm [2.8-14.9], $p = 0.316$), and V7 (4.5 mm [2.3-7.9] *vs*. 4.2 mm [2.3-8.3], $p = 0.318$) (Table 1). The proportion of patients with an inferior right hepatic vein

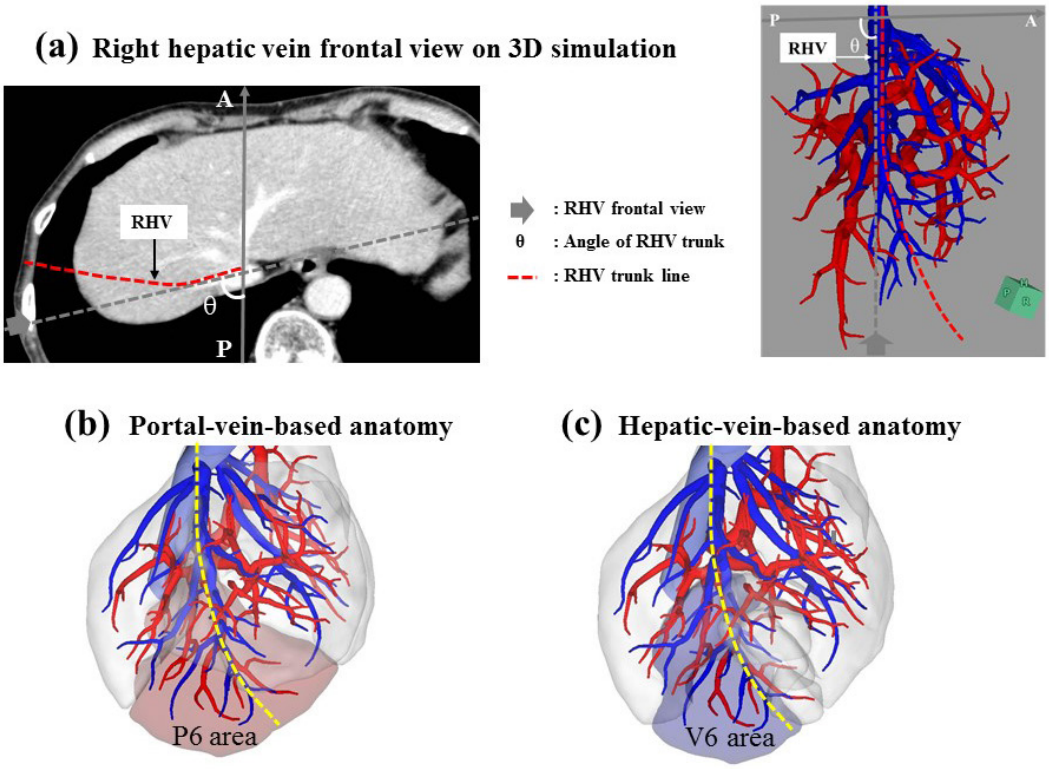

Figure 1. Definition of each anatomy in segment 6. (a) The frontal view was defined as the rotation angle (θ) between the RHV trunk and the median line on the inferior vena cava of the horizontal plane of the CT scan. The median angle (θ) of the basic trunk of the RHV was 83.3 degrees (range, 56.2-97.4 degrees) for all the patients. Three-dimensional simulation was always performed using the RHV frontal view. The basic line was drawn as the RHV trunk line when the RHV trunk was fully exposed as long as possible. The RHV trunk line was defined as the main trunk of the RHV fully exposed as long as possible. **(b, c)** The portal-vein-based segment(S) 6 and hepatic-vein-based S6 were expressed as the perfusion areas of the portal vein (P6) and drainage areas of the hepatic vein (V6), respectively, on the RHV trunk line of the 3D anatomy.

Table 1. Anatomic characteristics and tributary pattern of the hepatic vein

Items	All ($n = 103^{*}$)	S6-dominant ($n = 43$)	Non-differnce ($n = 57$)	*p* value**
Angle of RHV trunk (θ) (degree)***	83.3 (56.2-97.4)	80.8 (66.4-95.4)	84.2 (56.2-97.4)	0.177
RHV thickness (mm)***	6.5 (2.8-14.9)	6.5 (2.8-11.2)	6.6 (2.8-14.9)	0.316
V7 thickness to RHV (mm)***	4.3 (2.3-8.3)	4.5 (2.3-7.9)	4.2 (2.3-8.3)	0.318
Presence of IRHV, *n* (%)	56/103 (54.4)	31/43 (72.1)	25/57 (43.9)	0.008
V6 to MHV, *n* (%)	21/103 (20.4)	15/43 (34.9)	6/57 (10.5)	0.006
V8 to MHV, *n* (%)	48/103 (46.6)	22/43 (51.2)	26/57 (45.6)	0.687

*Include S5-dominant patients ($n = 3$); **S6-dominant *vs*. Non-difference; ***median (range). RHV = right hepatic vein; IRHV = inferior right hepatic vein; MHV = middle hepatic vein.

(IRHV) was significantly higher (72.1% *vs*. 43.9%, $p = 0.008$), and the proportion of patients with V6 of the MHV tributary was higher (34.9% *vs*. 10.5%, $p = 0.006$) in the S6-dominant group than in non-difference group. On the other hand, the presence of V8 of the MHV tributary ($p = 0.687$) did not differ significantly among the groups.

3.3. *Branch pattern of the portal vein*

Standard bifurcation was found in 93 patients, trifurcation in 3 patients, and other specific branch types of the main portal trunk were found in 7 patients. There was no significant difference in the normal branch pattern of the main portal trunk (S6-dominant group vs. non-difference group, 41 patients [95.3%] *vs*. 50 patients [87.7%], respectively, $p = 0.293$). In the 93 patients with the standard branch type, the length of the right portal trunk ($p = 0.439$) and anterior branch trunk ($p = 0.809$) did not differ significantly between the S6-dominant group and non-difference group (Table 2). In contrast, the median posterior branch was significantly shorter in the S6-dominant group than in the non-difference group (15.6 [0-44.3] *vs*. 18.7 mm [0-47.8], $p = 0.026$). The angle between the anterior and posterior trunks did not differ significantly between the S6-dominant group and non-difference group ($p = 0.479$). The number of branches of P6 also did not differ significantly ($p = 0.856$).

Regarding the branch patterns of the first P6, the S6-dominant group included a significantly higher proportion of the proximal type than the non-difference group (31 patients [72.1%] *vs*. 12 patients [27.9%]) (Figure 2). The non-difference group included a significantly higher proportion of the distal type than the S6-dominant group (10 patients [17.0%] *vs*. 47 patients [83.0%], $p < 0.001$).

4. *Volume analysis*

According to the perfusion area of each segment, the volumes of S6 (204 [69-366] *vs*. 152 mL [44-287], $p < 0.001$) and S7 (224 [82-561] *vs*. 205 mL [74-366], p

Table 2. Anatomic characteristics of the portal vein in standard bifurcation type cases ($n = 93$)

Items	All ($n = 93^{*}$)	S6-dominant ($n = 41$)	Non-differnce ($n = 50$)	p value**
Length of right portal vein trunk (mm)	23.6 (5.4-41.9)	23.8 (5.4-41.9)	22.4 (6.5-39.4)	0.439
Length of anterior branch trunk (mm)	16.3 (0-37.5)	16.1 (0-36.4)	16.1 (0-37.5)	0.809
Length of posterior branch trunk (mm)	17.2 (0-47.8)	15.6 (0-44.3)	18.7 (0-47.8)	0.026
Angle between anterior and posterior trunk (degrees)	71.4 (41.2-106.3)	71.6 (46.8-106.3)	71.4 (41.2-100.6)	0.479
Number of portal veins in segment 6	1 (1-3)	1 (1-3)	1 (1-3)	0.856

Data are expressed as the medians (range). *Include S5-dominant patients ($n = 2$); **S6-dominant *vs*. Non-difference.

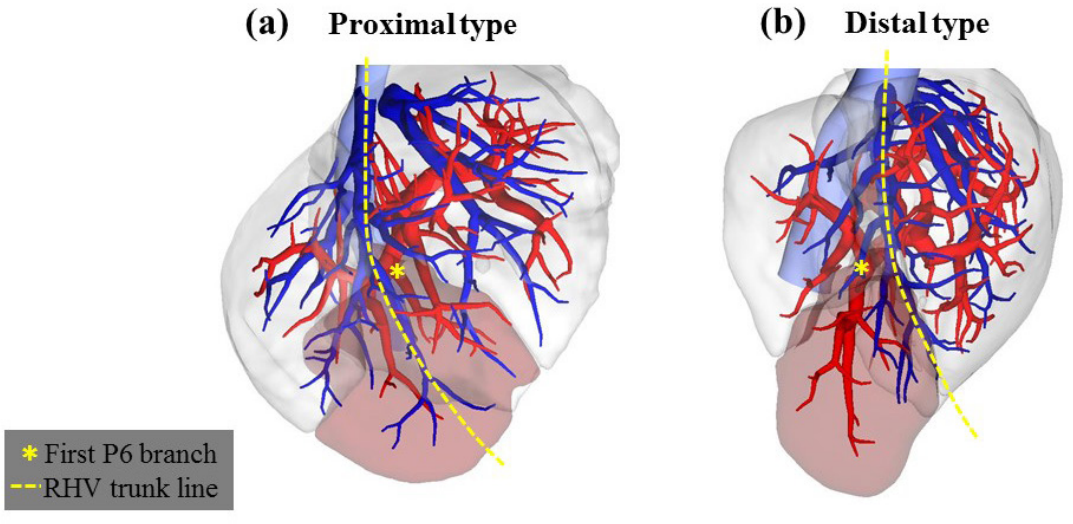

		Proximal type	Distal type	p value*
S6-dominant	(n=43) (%)	31 (72.1)	12 (27.9)	<0.001
Non-difference	(n=57) (%)	10 (17.0)	47 (83.0)	<0.001

* Fisher's exact test.

Figure 2. Branch pattern of the first portal vein in segment 6. (a) In the branch patterns of first P6, the S6-dominant group included a significantly higher proportion of the proximal type than the non-difference group on the RHV trunk line. **(b)** In contrast, the non-difference group included a significantly higher proportion of the distal type.

Table 3. Volume analysis of each segment in the right liver

Segment	All (n = 103*)	S6-dominant (n = 43)	Non-differnce (n = 57)	p value**
S5 (mL)	115 (33-360)	106 (33-312)	115 (39-360)	0.328
S6 (mL)	164 (44-366)	204 (69-366)	152 (44-287)	< 0.001
S7 (mL)	215 (74-561)	224 (82-561)	205 (74-366)	0.037
S8 (mL)	202 (43-536)	198 (45-536)	208 (43-464)	0.834

Data are expressed as the medians (range). *Include S5-dominant patients (n = 3); **S6-dominant *vs*. Non-difference.

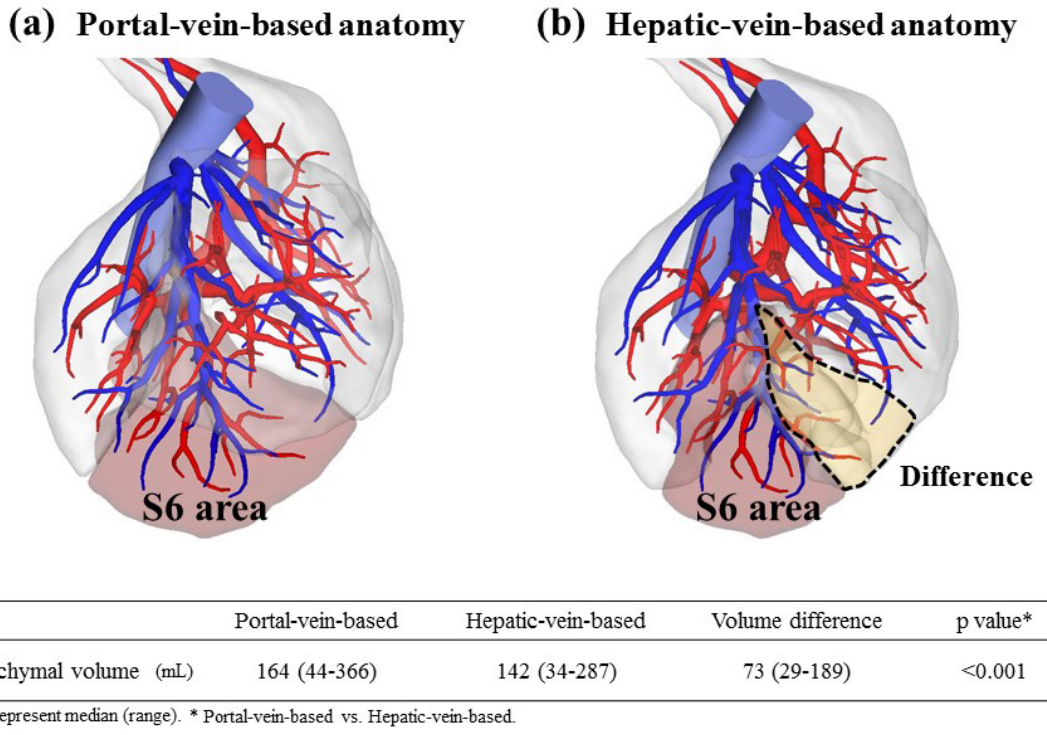

	Portal-vein-based	Hepatic-vein-based	Volume difference	p value*
Parenchymal volume (mL)	164 (44-366)	142 (34-287)	73 (29-189)	<0.001

Figures represent median (range). * Portal-vein-based vs. Hepatic-vein-based.

Figure 3. Volume difference in segment 6. (a, b) The portal-vein-based S6 was significantly larger than that derived from the hepatic-vein-based liver anatomy. The volume difference between the two groups was 73 mL [29-189 ml] in S6.

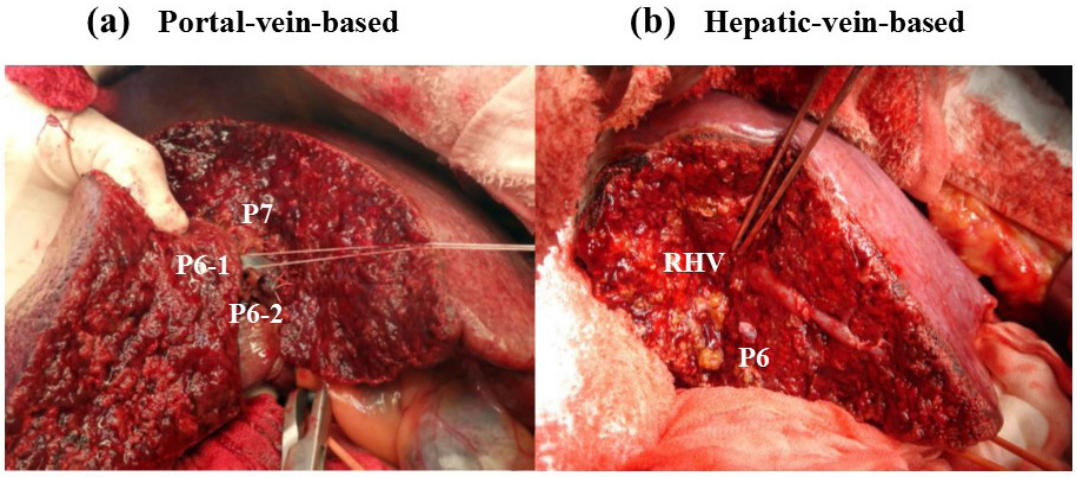

Figure 4. Liver transection based on each anatomy. (a) The portal-vein-based liver transection was performed. Two P6 branches were detected using dye injected into each branch of P6. Each P6 branch was divided at the root and P7 was preserved. No thick branch of RHV was visualized. **(b)** The hepatic-vein-based liver transection was performed in proximal branch type P6. The full length of RHV in S6 was exposed, while root of P6 was not visualized.

= 0.037) were significantly larger in the S6-dominant group than in the non-difference group (Table 3). However, there was no significant difference in S5 and S8 between the two groups. The median volume of the portal-vein-based anatomy of S6 (Figure 3a) was 164 mL (44-366 mL), while the median volume of the hepatic-vein-based anatomy of S6 (Figure 3b) was 142 mL (34-287 mL; $p < 0.001$). The median volume difference in S6 between the two groups was 73 mL (29-189 mL) (Figure 3).

5. *Liver transection in each model*

In the clinical technique, the portal-vein-based liver transections were performed using dye injected into two branch of P6 and the hepatic-vein-based liver transection was performed in proximal branch type of P6 (Figure 4a). In the portal-vein-based transection, each P6 branch was divided at the root and P7 was preserved. No thick branch of RHV was visualized at the transection site. The full length of RHV in S6 was exposed in the hepatic-vein-based transection. Thus, the root of P6 was not visualized because of proximal branch type of P6 (Figure 4b).

4. Discussion

This study showed that 41.7% of the segment planes in S6 did not match with the portal-vein-based and hepatic-vein-based 3D anatomies. The proximal branch type of P6 (72.1%) and the presence of the IRHV (72.1%) were conclusive factors for S6-dominant segmentation.

Several studies have mentioned the anatomical difference between the perfusion area of portal vein and drainage area of hepatic vein (*1,2,8*). However, objective rules for assessing this difference have not yet been established. The RHV frontal view in the present study can classify the branch pattern of P6 into the proximal or distal. In particular, the all proximal branch of P6 perfused the ventral side of the RHV, which is thought to correspond to S5 in the hepatic-vein-based anatomy. To understand these anatomic characteristics enables to perform more precise anatomic liver resection (*e.g.*; anatomic resection in less than subsegment). This novel rule might also apply to the other segmental planes in the liver parenchyma.

Transection of the liver parenchyma along with the major hepatic vein is considered to be one of the gold-standard methods for anatomic liver resection (*6,7*). However, present study revealed that the 41.7% was failed to remove entire perfusion area in S6 when the patients was performed based on the hepatic-vein-based anatomy. In contrast, the parenchymal staining method which established by Makuuchi is one of an anatomic liver resection. The dye is injected into the portal vein to determine the region that should be resected. This procedure can be contributed to resect potential metastases *via* the portal vein in the tumor-occupying segment (*14-16*). Therefore, in the presence of portal vein tumor thrombus, the portal-vein-based liver transection is a prefer procedure to avoid intrahepatic recurrence (*9*).

The S6-dominant group has two unique features on 3D. First, 72.1% of the patients had one or more IRHV. Second, 72.1% of the patients had a proximal branch of P6, which was supported by the result of a shorter posterior branch of the portal trunk. These findings reflect a large drainage area in the liver parenchyma as well as a wide perfusion area in the S6-dominant group. Therefore, the parenchymal volume in S6 was significantly larger in the S6-dominant group than that in the non-difference group.

The preoperative liver volume measurements based on 3D anatomy imaging have been shown to agree with the actual volume of the liver resected at operation (*17-19*). The median volume difference between the portal-vein-based and hepatic-vein-based anatomies in S6 was 73 mL. We believe this volume difference is large because the median parenchymal volume of S6 was 164 mL. Therefore, almost half of the liver volume was discordant between the portal-vein-based and hepatic-vein-based anatomies.

Few studies have thus far identified the factors accounting for the anatomical features between the portal and hepatic veins at liver surgery. The present study emphasized the priority of portal-vein-based anatomic liver resection when precise resection is required such as portal vein thrombus, intra sub segmental metastasis and smaller anatomic resection which depend on the each portal vein branch. We believe that taking this anatomic concept into careful consideration before operation may increase the patient's benefits in liver resection.

References

1. Kakazu T, Makuuchi M, Kawasaki S, Miyagawa S, Nakazawa Y, Kubota T, Takayama T, Kosuge T. Reconstruction of the middle hepatic vein tributary during right anterior segmentectomy. Surgery. 1995; 117:238-240.
2. Hashimoto T, Sugawara Y, Kishi Y, Akamatsu N, Matsui Y, Kokudo N, Makuuchi M. Reconstruction of the middle hepatic vein tributary in a right lateral sector graft. Liver Transpl. 2005; 11:309-313.
3. Mise Y, Hasegawa K, Satou S, Aoki T, Beck Y, Sugawara Y, Makuuchi M, Kokudo N. Venous reconstruction based on virtual liver resection to avoid congestion in the liver remnant. Br J Surg. 2011; 98:1742-1751.
4. Couinaud C. Surgical anatomy of the liver revised (Pers, ed.). Paris, France, 1989.
5. Couinaud C. Liver anatomy: Portal (and suprahepatic) or biliary segmentation. Dig Surg. 1999; 16:459-467.
6. Makuuchi M, Hasegawa H, Yamazaki S. Ultrasonically guided subsegmentectomy. Surg Gynecol Obstet. 1985; 161:346-350.

7. Shindoh J, Mise Y, Satou S, Sugawara Y, Kokudo N. The intersegmental plane of the liver is not always flat--tricks for anatomical liver resection. Ann Surg. 2010; 251:917-922.
8. Sato F, Igami T, Ebata T, Yokoyama Y, Sugawara G, Mizuno T, Nagino M. A study of the right intersectional plane (right portal scissura) of the liver based on virtual left hepatic trisectionectomy. World J Surg. 2014; 38:3181-3185.
9. Yamazaki S, Takayama T. Surgical treatment of hepatocellular carcinoma: Evidence-based outcomes. World J Gastroenterol. 2008; 14:685-692.
10. Hayashi Y, Takayama T, Yamazaki S, Moriguchi M, Ohkubo T, Nakayama H, Higaki T. Validation of perioperative steroids administration in liver resection: A randomized controlled trial. Ann Surg. 2011; 253:50-55.
11. Yamazaki S, Takayama T, Kimura Y, Moriguchi M, Higaki T, Nakayama H, Fujii M, Makuuchi M. Transfusion criteria for fresh frozen plasma in liver resection: A 3 + 3 cohort expansion study. Arch Surg. 2011; 146:1293-1299.
12. Yamazaki S, Takayama T, Moriguchi M, Mitsuka Y, Okada S, Midorikawa Y, Nakayama H, Higaki T. Criteria for drain removal following liver resection. Br J Surg. 2012; 99:1584-1590.
13. Mise Y, Satou S, Shindoh J, Conrad C, Aoki T, Hasegawa K, Sugawara Y, Kokudo N. Three-dimensional volumetry in 107 normal livers reveals clinically relevant inter-segment variation in size. HPB (Oxford). 2014; 16:439-447.
14. Takayama T, Makuuchi M, Watanabe K, Kosuge T, Takayasu K, Yamazaki S, Hasegawa H. A new method for mapping hepatic subsegment: Counterstaining identification technique. Surgery. 1991; 109:226-229.
15. Makuuchi M, Hashikura Y, Kawasaki S, Tan D, Kosuge T, Takayama T. Personal experience of right anterior segmentectomy (segments V and VIII) for hepatic malignancies. Surgery. 1993; 114:52-58.
16. Torzilli G, Procopio F, Cimino M, Del Fabbro D, Palmisano A, Donadon M, Montorsi M. Anatomical segmental and subsegmental resection of the liver for hepatocellular carcinoma: A new approach by means of ultrasound-guided vessel compression. Ann Surg. 2010; 251:229-235.
17. Yamanaka J, Saito S, Fujimoto J. Impact of preoperative planning using virtual segmental volumetry on liver resection for hepatocellular carcinoma. World J Surg. 2007; 31:1249-1255.
18. Li YC, Hu Y, Zhang MM, Jin XQ, Fan X, Pu CL, Guo CB, Kang Q, Dai XK, Deng YH. Usage of 64-detector-row spiral computed tomography volumetry in preoperative volume prediction in living donor liver transplantation in children. Pediatr Surg Int. 2011; 27:445-449.
19. Takamoto T, Hashimoto T, Ogata S, Inoue K, Maruyama Y, Miyazaki A, Makuuchi M. Planning of anatomical liver segmentectomy and subsegmentectomy with 3-dimensional simulation software. Am J Surg. 2013; 206:530-538.

(Received March 13, 2017; Revised April 12, 2017; Accepted April 13, 2017)